Catalysis Today 236 (2014) 98–107

Contents lists available at ScienceDirect

Catalysis Today

journal homepage: www.elsevier.com/locate/cattod

# PVA composite catalytic membranes for hyacinth flavour synthesis in a pervaporation membrane reactor

T.F. Ceia[a], A.G. Silva[a], C.S. Ribeiro[a], J.V. Pinto[b], M.H. Casimiro[a], A.M. Ramos[a], J. Vital[a,*]

[a] REQUIMTE/CQFB, Departamento de Química, Faculdade de Ciências e Tecnologia, FCT, Universidade Nova de Lisboa, 2829-516 Caparica, Portugal
[b] Departamento de Ciência dos Materiais and CENIMAT/I3N, Faculdade de Ciências e Tecnologia, FCT, Universidade Nova de Lisboa, 2829-516 Caparica, Portugal

ARTICLE INFO

*Article history:*
Received 5 August 2013
Received in revised form 12 February 2014
Accepted 14 February 2014
Available online 3 April 2014

*Keywords:*
Biorefinery
Hyacinth flavour
Acetalization
Polymeric catalytic membrane reactor
PVA membrane
Pervaporation

ABSTRACT

Composite catalytic membranes consisting of poly(vinyl alcohol) cross-linked with glutaraldehyde and H-USY zeolite dispersed into the polymeric matrix were prepared and used in the hyacinth flavour synthesis by acetalization of phenylacetaldehyde and glycerol.

In order to study the effects of catalyst loading, polymer cross-linking and hydrophilic/hydrophobic balance in the catalytic behaviour of the prepared membranes, catalytic runs were performed in batch conditions and in a pervaporation assisted catalytic membrane reactor. It was found that polymer cross-linking strongly affects the membranes' sorption and transport properties which seem to improve with the increase of catalyst loading. Results also evidence that permeation in membrane reactor was well accomplished with good selectivity to water.

The catalytic membranes were characterized by measurement of thickness, water contact angles and swelling degree as well as by Fourier transform infrared spectroscopy (FTIR), atomic force microscopy (AFM) and scanning electron microscopy (SEM).



## 1. Introduction

The use of aromatic chemicals as flavouring compounds has been growing since the chemical developments that allowed their synthesis and commercial production. To be able to be used without hazard to public health these fragrances must be included in approved official lists of naturally occurring or synthetically produced flavouring substances (e.g.: the FEMA-GRAS list regulated by the Food and Drug Administration) [1]. Among the approved fragrances, hyacinth flavour, a high value product used in food and cosmetic industry, is generally synthetized by acetalization of phenylacetaldehyde with glycerol (Scheme 1) under acid catalysis.

Glycerol is a by-product of the biodiesel manufacturing process by transesterification of vegetable oils or animal fats [2]. Currently, as the global research is focused on the development of sustainable and renewable resources, the production of biodiesel has been increasing significantly leading to glycerol amounts larger than the market can absorb. In order to develop new uses for glycerol different catalytic processes, including oxidation, reforming, hydrogenolysis, etherification, esterification and acetalization reactions, have been reported in the transformation of glycerol [3–6]. In the particular case of the reaction in study, the major environmental and economic gains of the phenylacetaldehyde acetalization reaction are the glycerol effective reuse in the biorefineries and the conversion of glycerol to a value added chemical [3].

In general acetals are prepared through a reversible reaction between an alcohol and an aldehyde with water as a by-product. The thermodynamic limitations in conventional reaction systems result in low conversions for these reactions [7,8]. In order to displace equilibrium and improve reaction conversion, reactive azeotropic distillation has been proposed for removal the water formed in the acetalization reaction [1]. However this technique requires large amounts of toxic solvents, oversized equipment and consequently leads to high energetic costs.

The use of catalytically active membranes and in particularly the use of polymeric catalytic membrane reactors (PCMRs), can offer specific advantages by combining in a single unit operation chemical reaction and separation [9–11]. Moreover, the continuous removal of water from the reaction mixture by means of pervaporation coupling shifts the reaction to the product side and thus increases the yield [12–15]. Other beneficial aspects associated to PCMRs include the low energy consumption and the possibility of

* Corresponding author. Tel.: +351 21 2948385; fax: +351 21 2948350/+351 21 2948550.
*E-mail address:* jsmv@fct.unl.pt (J. Vital).

http://dx.doi.org/10.1016/j.cattod.2014.02.052
0920-5861/

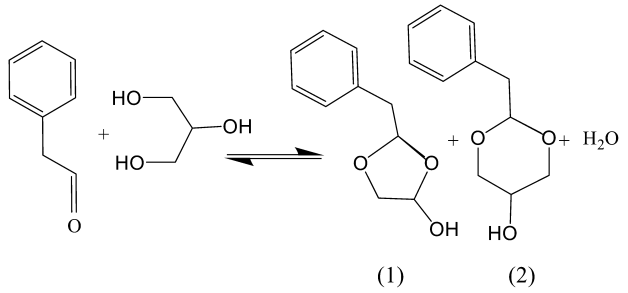


**Scheme 1.** Acetalization of phenylacetaldehyde with glycerol. (1) 2-Benzyl-4-hydroxy methyl-1,3-dioxan. (2) 2-Benzyl-5-hydroxy-1,3-dioxane.

carrying out the reaction without the use of solvents and thus render the process environmentally and technically more attractive.

Although high conversions can be achieved in the acetalization of glycerol and phenylacetaldehyde when very pure reactants are used, the use of cheap low grade glycerol with relatively high water content, is desirable. However, under these conditions equilibrium conversion decreases significantly becoming mandatory the removal of water simultaneously with the chemical reaction. In the present work, catalytic composite membranes consisting in poly(vinyl alcohol) (PVA) cross-linked with glutaraldehyde (Scheme 2) and zeolite HUSY dispersed into the polymeric matrix, were prepared and used in the acetalization of phenylacetaldehyde. Catalytic runs were performed in batch conditions and in pervaporation assisted catalytic membrane reactor. The effects of catalyst loading, polymer cross-linking and hydrophilic/hydrophobic balance in the catalytic behaviour of the prepared membranes were evaluated, as well as the application of a pervaporation catalytic membrane reactor as an alternative method to azeotropic distillation.

## 2. Experimental

### 2.1. Preparation of catalytic composite membranes

PVA (Aldrich, ≥99% hydrolyzed) was dissolved in water at 80 °C, during 2 h. In order to obtain membranes with different catalyst loadings and different cross-linkings, the appropriated amounts of H-USY zeolite (Zeolyst, CBV 720, average particle size: 0.8 μm) were suspended in 20 mL of aqueous 8 wt% PVA solution, sonicated for 1 h and then mixed with the appropriated amount of glutaraldehyde (GA) (Aldrich, aqueous solution, 50 wt%).

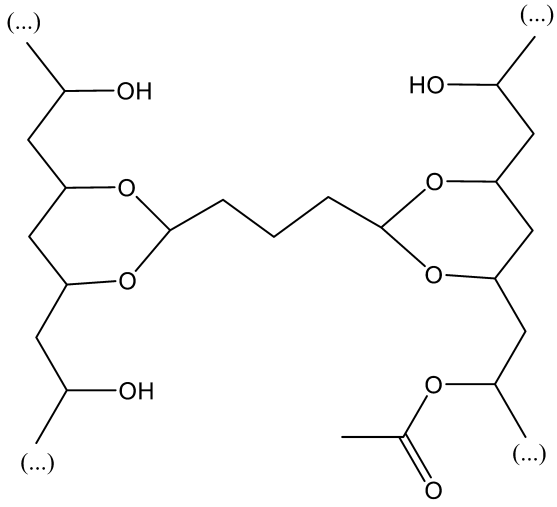


**Scheme 2.** PVA cross-linked with glutaraldehyde and partially acetylated.

The solutions were poured in a Petri dish and allowed to concentrate and cross-link at 40 °C for 135 min after what phase inversion was obtained by adding methanol to the Petri dish. Finally the membranes were removed from the Petri dish and allowed to dry overnight at room temperature.

PVA acetylation was carried out by reaction with acetic anhydride (>99%, Riedel-de Haën) at 110 °C and atmospheric pressure during 24 h, followed by acetone extraction and drying at 80 °C for 4 h. The partly acetylated PVA was then subjected to the procedure previously described for membrane preparation. The code Y*u*G*v*A*cw* means a PVA matrix *v*% cross-linked with glutaraldehyde, loaded with *u*% of H-USY zeolite (weight of H-USY/weight of PVA) and *w*% acetylated. The *v*% cross-linking means that was added to the PVA aqueous solution an amount of glutaraldehyde corresponding to *v*/4% of the total number of moles of the PVA OH groups, assuming that each mole of glutaraldehyde acetalizes 4 mol of PVA OH groups. The *w*% acetylation means that the parent PVA was treated with an amount of acetic anhydride corresponding to *w*% of the total number of moles of the PVA OH groups.

### 2.2. Membranes' characterization

The catalytic membranes were characterized by measurement of thickness, water contact angle and swelling degree as well as by Fourier transform infrared spectroscopy (FTIR), atomic force microscopy (AFM) and scanning electron microscopy (SEM).

Membranes' thickness was measured using a Braive Instruments micrometer (0.001 mm accuracy) and water contact angles were measured using a CAM 100 series 110057 goniometer. Solvent absorption experiments were carried out by immersing dry samples of the obtained membranes in the appropriate reagent (water, glycerol or phenylacetaldehyde) for 24 h at room temperature. Then membranes were removed, the excess of reagent wiped out from the its surface and weighted.

FTIR spectra were obtained in transmission mode by using KBr pellets in a Perkin-Elmer FT-IR Spectrum 1000 spectrophotometer (40 times scanning; 4 $cm^{-1}$ of resolution).

The surface morphology was investigated by atomic force microscopy (AFM) using an Asylum MFP-3D Microscope in AC mode. Scanning electron microscopy (SEM) was performed on a Hitachi S-2400 equipment.

### 2.3. Catalytic experiments

The synthesis of hyacinth flavour was performed in batch conditions and in a pervaporation assisted catalytic membrane reactor using the prepared composite catalytic membranes.

Catalytic tests in batch conditions were carried out in a jacketed batch reactor at 100 °C using the catalytic membranes cut in 0.6 cm diameter disks. In a typical experiment the reactor was loaded with 14 mL of glycerol (99%, Sigma-Aldrich), a known amount of membrane's mass (0.5–0.8 g), 12 mL of phenylacetaldehyde (>95%, Sigma-Aldrich) and 1 mL of undecane (analytical standard, Fluka) as GC internal standard for gas chromatography (GC).

The experiments with free H-USY were performed at 100 °C, 110 °C, 120 °C and 140 °C with the reactor loaded with 0.1 g of catalyst, and the same amounts of the other components. Samples were taken at regular time periods and analyzed by GC.

Catalytic runs in membrane reactor operating under sweep gas pervaporation conditions were performed using a reactor composed of two metal slabs, each having an inlet and an outlet, as described in a previous work [20]. The membrane was assembled in such a way that the catalytic layer side (i.e. the side facing the glass in the Petri dish, during preparation) was facing the reactants chamber.

The reactor was heated at 70 °C and the reaction mixture (45 mL of glycerol, 19.5 mL of phenylacetaldehyde and 12.7 mL of undecane) was pumped at 12.4 mL/min. Dry nitrogen gas (flow rate of 170 mL/min), was used to sweep the downstream side of the membrane into 70 mL of acetic anhydride. In order to quantify permeated water, samples from this solution were prepared by adding 1 mL of *n*-propanol and 0.1 mL of *n*-nonane (GC standard) to 0.1 mL of the permeated solution and analyzed by GC.

## 3. Results and discussion

### 3.1. Characterization of the catalytic membranes

The experimental methodology developed allowed to obtained PVA composite catalytic membranes morphologically reproducible. All the membranes used in the both catalytic tests (batch and membrane reactor) had similar appearance presenting thickness and weight values (average and standard deviation) of $0.25 \pm 0.02$ mm and $1.67 \pm 0.05$ g, respectively.

#### 3.1.1. Solvent absorption and water contact angle

The membranes' swelling (taken as solvent absorption) degree ($Q_r$) was calculated using the expression:

$$Q\,(\%) = \frac{m - m_0}{m_0} \times 100 \quad (1)$$

where $m$ is the mass of the swollen sample and $m_0$ is the initial mass.

Membrane's swelling reaches much higher values in water than in glycerol or phenylacetaldehyde (Table 1) not only due to the hydrophilic character of PVA but also due to the small size of the water molecules, which can easily diffuse into the free volumes of the PVA matrix.

Swelling with glycerol or phenyl acetaldehyde increases with the increase of the catalyst loading, probably due to the increase of the matrix free volume and due to voids formation. However, swelling with water only increases when the catalyst loading increases from 5% to 10%, decreasing for higher loadings. A possible explanation is the possibility of the catalyst particles act as spacers, restricting the movement of the polymer chains beyond certain limits.

The catalyst loading appears to have no effect on the hydrophilicity of the membranes since significant changes are not observed in the water contact angle when the catalyst load increases.

The increase of polymer cross-linking appears to lead to an increase in the hydrophobicity of the membranes, in agreement with the results reported by other authors [16], not only because the membrane swelling in water decreases but also because the water contact angle increases when the polymer cross-linking increases. The effects of the polymer cross-linking on the membranes swelling in glycerol or phenylacetaldehyde are not conclusive.

In agreement with observations previously reported [17] the increase in membrane acetylation appears also to lead to the increase of membrane hydrophobicity since the membrane swelling in water decreases and simultaneously the water contact angle of the membranes increases when membrane acetylation increases.

#### 3.1.2. FTIR spectroscopy

The changes in the PVA chemical structure were evaluated by FTIR spectroscopy. Fig. 1 shows the FTIR spectra obtained for PVA membranes with different cross-linking degrees. All spectra exhibit the major peaks related to the typical PVA pattern (a O–H stretching broad band around 3550–3200 $cm^{-1}$, a C–H stretch vibration band around 3000–2840 $cm^{-1}$ and a $CH_2$ deformation band at

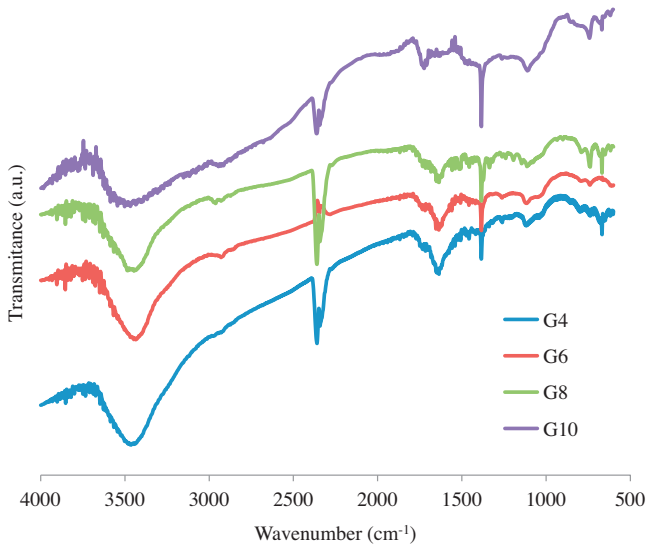


**Fig. 1.** FTIR spectra of membranes Y10G04, Y10G06, Y10G08 and Y10G10. Effect of glutaraldehyde addition.

1461–1417 $cm^{-1}$ [18]), together with the acetal bridge C–O–C peak at 1150–1085 $cm^{-1}$ resulting from the reaction between PVA and GA. The presence of a small band at 1750–1735 $cm^{-1}$ can be assigned to the C=O stretching from the acetate remaining from PVA (poly(vinyl alcohol) is obtained by hydrolysis of poly(vinyl acetate)) or from incomplete cross-linking reaction with GA since as a bifunctional cross-linker, one of the GA aldehyde groups may react with hydroxyl groups of a PVA polymer chain by forming a acetal or hemi-acetal, while the other one might not react due to some conformation limitations [18].

Additionally, to confirm the effectiveness of cross-linking reaction a semiqualitative analysis was performed by comparing the absorbance ratios between the bands assigned to acetal (C–O–C) or carbonyl (C=O) groups and the characteristic band of the OH group, taken at the maximum absorbance wavenumber (Fig. 2A). As expected, the absorbance ratio C–O–C/OH increases when the nominal cross-linking increases. These results are in agreement with the observed increase of membrane hydrophobicity with the amount of GA added (Table 1) suggesting a decrease of the amount of PVA OH groups and, therefore, an increase of cross-linking.

Simultaneously with the increase of the C–O–C/OH absorbance ratio it is observed an increase of the C=O/OH absorbance ratio indicating an increasingly incomplete cross-linking reaction when the amount of added cross-linker increases.

Concerning acetylation results, it was found an increase of the C=O/OH ratio with the increase of the amount of added acetic anhydride (Fig. 2B), which suggests the increase of PVA acetylation.

#### 3.1.3. Membrane morphology

Membranes' morphology was examined by SEM and AFM. The SEM images representative for the morphology of the PVA composite catalytic membranes surface are depicted in Fig. 3. It can be clearly identified (Fig. 3B) an asymmetric membrane with two distinct layers: a selective layer made of a dense PVA layer, and a catalytic one composed of catalyst discrete particles dispersed on the bottom of the membranes' cross section.

AFM analysis (Fig. 4) reveals a possible correlation between the average roughness ($R_a$) and membrane's hydrophobicity. A possible interpretation is that the increase of membranes' hydrophilicity (lower cross-linking and acetylation degrees) can lead to higher water content in the polymeric matrix, which leads to membranes' increased plasticity thus reducing its surface roughness. In fact,

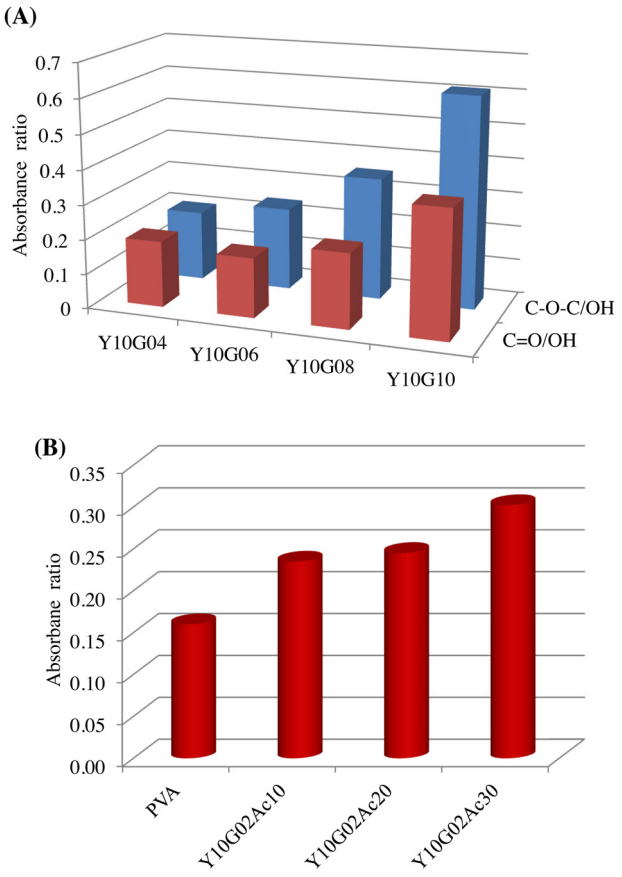


**Fig. 2.** Absorbance ratio between the bands assigned to acetal (C–O–C) or carbonyl groups (C=O) and OH groups: (A) PVA membranes with different polymer cross-linkings (C–O–C/OH); (B) PVA membranes with different acetylation degrees (C=O/OH).

there have been reports of other authors on the effects of traces of good polymer solvents, leading to flatter surfaces [19]. Simultaneously, higher amounts of H-USY zeolite lead also to lower roughness values. Using the same interpretation, this effect is likely to be due to the zeolite's hydrophilic character.

### 3.2. Catalytic tests

#### 3.2.1. Batch experiments

In order to evaluate the effect of the catalyst loading, polymer cross-linking and the PVA acetylation on the catalytic performance of the composite membranes, catalytic runs of acetalization

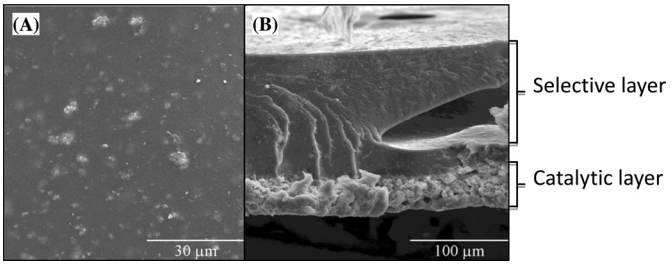


**Fig. 3.** SEM micrographs of Y10G02: (A) surface of the selective layer side; (B) cross section.

of phenylacetaldehyde and glycerol were performed in batch conditions.

As an example, Fig. 5 shows the conversion profiles obtained with the membranes prepared with different cross-linking degrees, for a same catalyst loading (Y10G04, Y10G06, Y10G08 and Y10G10).

A common feature to all concentration profiles is an initial induction period, which seems to increase when cross-linking increases. Such behaviour suggests an autocatalytic effect which can be justified by the improved transport properties of the membrane as a consequence of the interaction of acetal molecules with the polymer chains. In fact the acetal molecules can be intercalated between the PVA chains, decreasing the interchain hydrogen bonding.

Fig. 6 shows the conversion profiles obtained with free H-USY for the reaction carried out at 100 °C and using 99% pure glycerol (main graphic) as well as for the reaction carried out at 70 °C and using 87% pure glycerol (insertion). It is quite clear that in the last reaction conditions, when the lower grade glycerol is used, equilibrium conversion remains below 90%.

The fitting of a diffusion-kinetic model assuming fickian transport across the membrane and dependence of the diffusivity of phenylacetaldehyde on the concentration of the formed acetal fits quite well the kinetic data (solid lines) supporting that hypothesis.

### 3.3. Membrane modelling

#### 3.3.1. Basic assumptions

For modelling purposes the membranes were assumed as dense, homogeneous and symmetrical. The kinetic-diffusion model established was based on the following assumptions similar to those used in previous works [17,20–22] and works of other authors [23–27]:

- Isothermal and isobaric reaction conditions.
- Pseudo-steady state conditions for diffusion and reaction in the membrane.

**Table 1**
Membrane characterization.

| Membrane | Thickness (mm) | Swelling (%) | | | Contact angle (°) |
|---|---|---|---|---|---|
| | | Water | Glycerol | Phenylacetaldehyde | |
| Y05G02 | 0.237 | 255 | 23 | 11 | 55.94 |
| Y10G02 | 0.238 | 280 | 45 | 23 | 54.05 |
| Y15G02 | 0.238 | 229 | 55 | 29 | 66.69 |
| Y20G02 | 0.262 | 211 | 83 | 31 | 55.96 |
| Y10G04 | 0.246 | 268 | 15 | 25 | – |
| Y10G06 | 0.263 | 218 | 15 | 18 | 52.00 |
| Y10G08 | 0.247 | – | 43 | 15 | 56.09 |
| Y10G10 | 0.254 | 215 | 31 | 18 | 57.25 |
| Y10G02Ac10 | 0.284 | 278 | 115 | 20 | 56.36 |
| Y10G02Ac20 | 0.250 | 232 | 91 | 16 | 59.86 |
| Y10G02Ac30 | 0.249 | 228 | 104 | 20 | 61.60 |

Thickness, water contact angle and swelling in water, glycerol and phenylacetaldehyde.

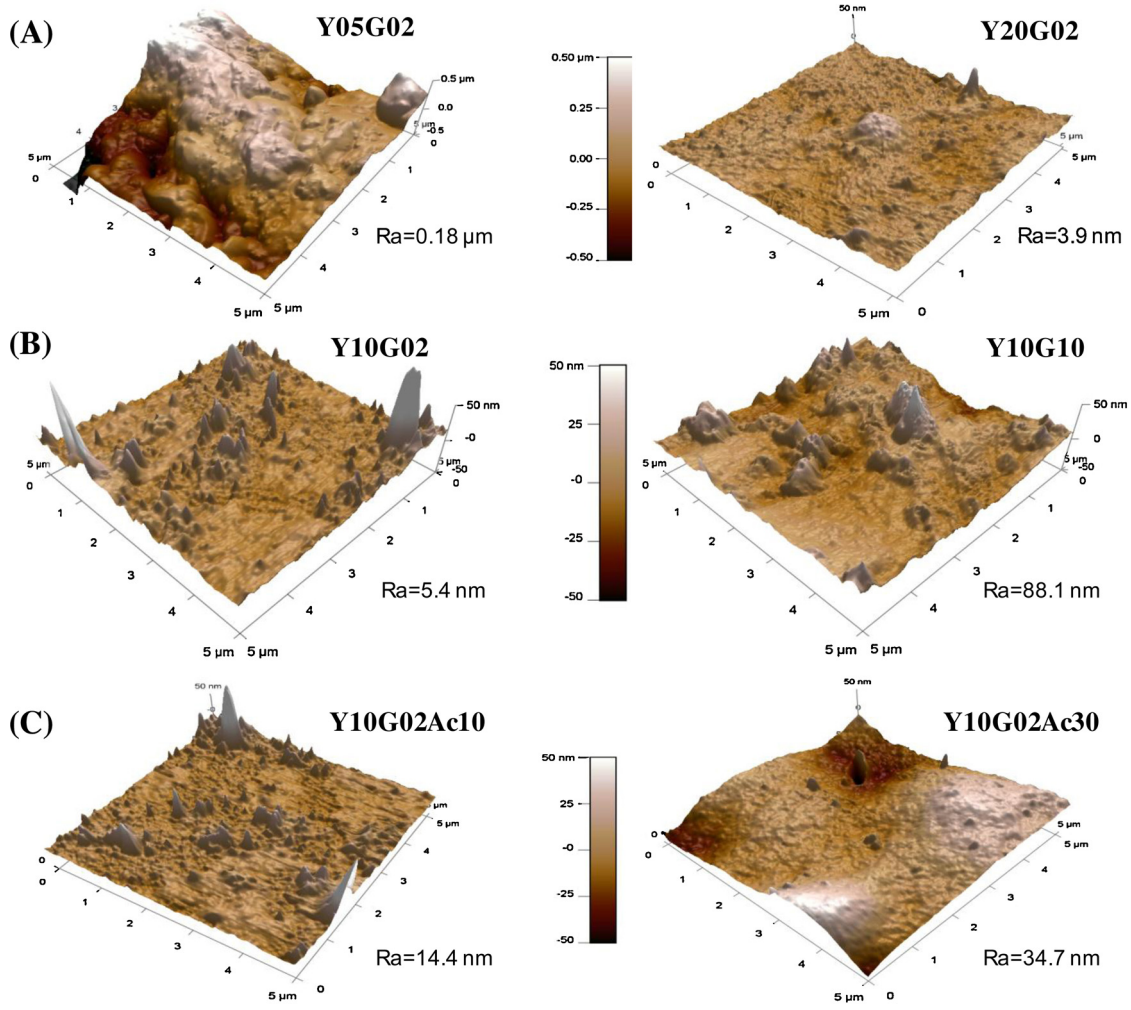


**Fig. 4.** 3D AFM images of PVA membranes with different: (A) catalyst loading (H-USY zeolite); (B) crosslinking degree; (C) acetylation degree.

- Unidirectional diffusion.
- Fickian transport across the membrane.
- Linear sorption equilibrium isotherm between the liquid phase and the membrane.

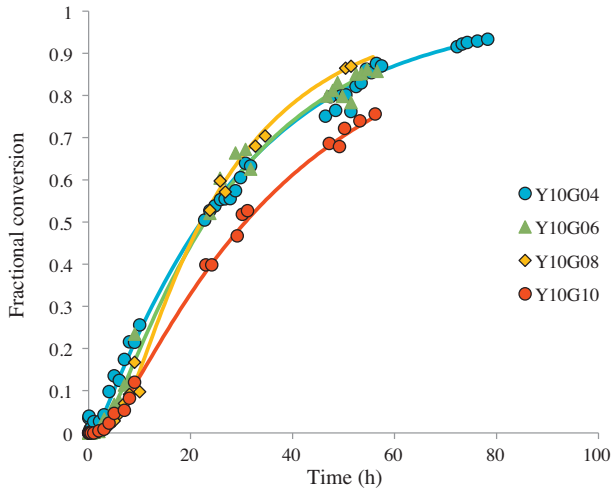


**Fig. 5.** Acetalization of phenylacetaldehyde and glycerol catalyzed by PVA/H-USY composite membranes. Conversion profiles obtained for membranes with increasing cross-linking degrees.

- Zero transport resistance for both reactants from the bulk phase to the membrane surface.
- Diffusivity of glycerol is assumed to be high compared to that of phenylacetaldehyde and set to a value high enough to become the model insensitive to the parameter.
- Diffusivity of phenylacetaldehyde is assumed to depend on the acetal concentration in the homogeneous liquid phase, $C_C^l$, according to the equation:

$$D_e = D_{e0} e^{\left(\frac{\alpha C_C^l}{\gamma C_C^l + \beta}\right)} \quad (2)$$

where $D_{e0}$ is the phenylacetaldehyde initial diffusivity; $\alpha$, $\beta$ and $\gamma$ are factors that influence diffusivity behaviour: $\alpha$ is the diffusivity-enhancing factor, $\beta$ is related with the extension of reaction induction period and $\gamma$ limits the diffusivity expansion.

### 3.3.2. Rate equation

In order to find a rate law catalytic tests with free H-USY were performed in five replicated experiments. Seven different kinetic models assuming 2nd order reversible reaction were tested, namely the pseudo-homogeneous model (PH), Langmuir-Hinshelwood assuming that the rate limiting step is the reactant adsorption (LH-RA), the surface reaction (LH-SR) or the product desorption (LH-PD) and Eley-Rideal also assuming that the rate limiting step is the reactant adsorption (ER-RA), the surface

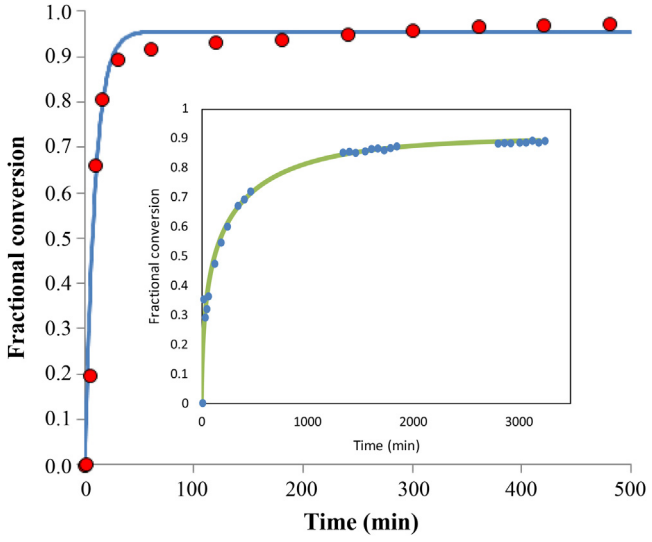


**Fig. 6.** Acetalization of phenylacetaldehyde and glycerol catalyzed by free H-USY at 100 °C and using 99% pure glycerol. Fitting of the LH-SR kinetic model to experimental data. The insertion corresponds to the same reaction carried out at 70 °C and using 87% pure glycerol.

reaction (ER-SR) or the product desorption (ER-PD). LH-SR was found as the best model by using variance analysis according to Kittrell [28], being the rate law in the range 373–403 K given by Eqs. (4)–(10):

$$-r'_A = k C_{A0}^2 \left\{ \frac{(1-X)\left(\theta_B - X\right) - X^2/Ke}{\left[1 + K_A C_{A0}(1-X) - K_B C_{A0}\left(\theta_B - X\right) + K_C C_{A0} X + K_D C_{A0} X\right]^2} \right\} \quad (4)$$

$$k = 2.5222\, e^{-851.767/T} \quad (5)$$

$$Ke = 832590\, e^{-\frac{4716.07}{T}} \quad (6)$$

$$K_A = 7.59 \times 10^{-7}\, e^{+4872.56/T} \quad (7)$$

$$K_B = 0.1013\, e^{-628.84/T} \quad (8)$$

$$K_C = 0.0321\, e^{-177.76/T} \quad (9)$$

$$K_D = 0.0069\, e^{-139.07/T} \quad (10)$$

where $X$ is fractional conversion, $C_{A0}$ is the initial concentration of phenylacetaldehyde and $\theta_B = C_{B0}/C_{A0}$ is the ratio of the initial concentrations of glycerol ($B$) and phenylacetaldehyde ($A$). The results of the variance analysis are shown in Table 2.

Fig. 6 shows the fitting of the LH-SR kinetic model to data obtained with the free H-USY.

### 3.3.3. Mole balances to the membrane

The mole balance of component $A$ over a differential element of depth d$z$ in pseudo-steady state conditions may be written as:

$$\frac{d^2 C_A}{dz^2} + \frac{\rho_{memb}}{D_e} r_A = 0 \quad (11)$$

being $D_e$ the phenylacetaldehyde diffusivity, $\rho_{memb}$ the membrane density and $r_A$ the reaction rate relative to phenylacetaldehyde.

### 3.3.4. Mole balances to the reactor

For batch reactor the mole balance equations may be written as:

$$\frac{dC_A^l}{dt} = -\frac{W}{V} R_A^{obs} \quad (12)$$

$$\frac{dC_B^l}{dt} = -\frac{W}{V} R_A^{obs} \quad (13)$$

$$\frac{dC_C^l}{dt} = -\frac{W}{V} R_A^{obs} \quad (14)$$

$$\frac{dC_D^l}{dt} = -\frac{W}{V} R_A^{obs} \quad (15)$$

where $C_A^l$, $C_B^l$, $C_C^l$, and $C_D^l$ are the concentrations in the liquid phase of phenylacetaldehyde, glycerol, acetal and water, respectively; $W$ is the weight of zeolite in the membrane used in the reaction and $V$ *is* the volume of the reaction mixture. $R_A^{obs}$ is the observed rate reaction relative to phenylacetaldehyde defined as:

$$R_A^{obs} = \frac{\int_0^L r'_A dz}{L} \quad (16)$$

where $L$ is the membrane half thickness.

### 3.3.5. Definition of boundary conditions

The concentrations of phenylacetaldehyde ($A$) and glycerol ($B$) on the membrane surfaces ($z = \pm L$) are obtained from:

$$C_A^S = K_A^{sorp} C_A^l \quad (17)$$

$$C_B^S = K_A^{sorp} C_B^l \quad (18)$$

where $K_i^{sorp}$ is the sorption coefficients of component $i$ in the membrane, calculated from the swelling data (Table 1).

**Table 2**
Variance analysis for kinetic model selection.

| Kinetic model | | Sum of squares | Degrees of freedom | Variance | Variance ratio | Critical $F$-value |
|---|---|---|---|---|---|---|
| | Pure error | 0.18058 | 56 | 0.00322 | | |
| PH | Residuals | 0.42151 | 68 | 0.00620 | 6.226 | 3.702 |
| | Lack-of-fit | 0.24093 | 12 | 0.02008 | | |
| LH-RA | Residuals | 0.36156 | 65 | 0.00556 | 6.236 | 4.138 |
| | Lack-of-fit | 0.18098 | 9 | 0.02011 | | |
| LH-SR | Residuals | 0.30020 | 65 | 0.00462 | 4.122 | 4.138 |
| | Lack-of-fit | 0.11962 | 9 | 0.01329 | | |
| LH-PD | Residuals | 0.34229 | 65 | 0.00527 | 5.572 | 4.138 |
| | Lack-of-fit | 0.16171 | 9 | 0.01797 | | |
| ER-RA | Residuals | 0.36156 | 65 | 0.00556 | 6.236 | 4.138 |
| | Lack-of-fit | 0.18098 | 9 | 0.02011 | | |
| ER-SR | Residuals | 0.33895 | 65 | 0.00521 | 5.457 | 4.138 |
| | Lack-of-fit | 0.15837 | 9 | 0.01760 | | |
| ER-PD | Residuals | 0.34229 | 65 | 0.00527 | 5.241 | 4.138 |
| | Lack-of-fit | 0.15649 | 9 | 0.01739 | | |

Pure error and residuals were taken as the differences between the experimental conversion values and its average or the value calculated by the model, respectively, for each value of time, for five replicated experiments. The lack-of-fit sum of squares is the difference between the sum of squares of residuals and pure error. The critical $F$-values were obtained for $\alpha = 0.0004$.

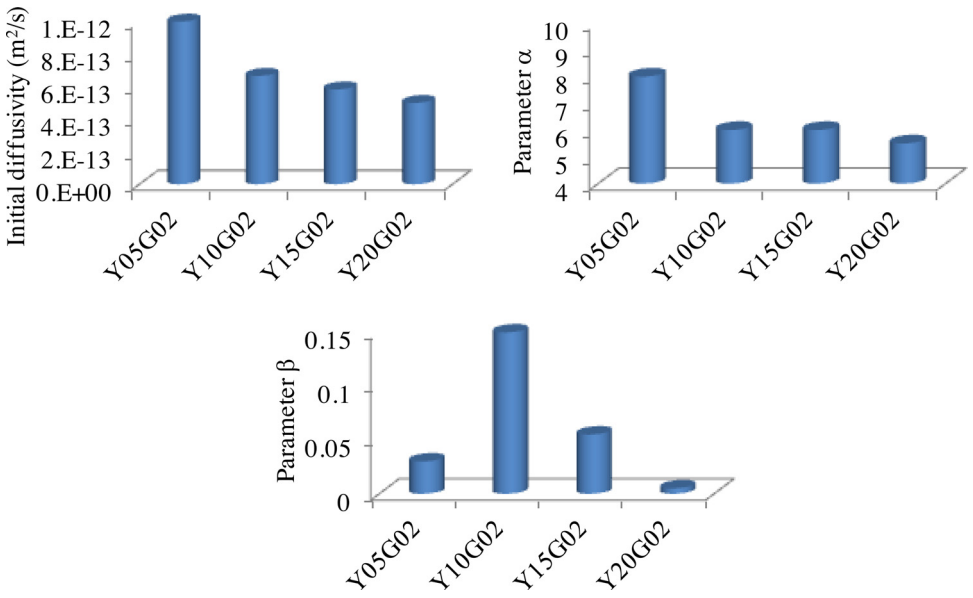


**Fig. 7.** Effect of H-USY loading on model parameters.

On the other hand in the membrane centre ($z = 0$) the reactant concentrations achieve a minimum value:

$$\frac{dC_A}{dz} = 0 \quad (19)$$

$$\frac{dC_B}{dz} = 0 \quad (20)$$

### 3.3.6. Model parameters

The model was fitted to the data points of concentration profiles obtained with the membranes described in Table 1, by changing the parameters $De_0$, $\alpha$, $\beta$ and $\gamma$.

### 3.3.7. Modelling calculations

A MATLAB™ program was developed for solving numerically the differential Eqs. (5)–(15) with the boundary conditions (17)–(20) and for estimating the unknown parameters. The parameter estimation algorithm consisted of a standard minimisation of the sum of squared errors employing the Levenberg–Marquardt optimization algorithm. The integration of the reactor mole balance Eqs. (12)–(15) was performed using the Euler method due to the high CPU requirements.

The calculation of the observed reaction rate $R_A^{obs}$ requires the integration of the membrane material balance Eq. (11). This second integration over the spatial coordinate $z$ is embedded in the first time integration of Eqs. (12)–(15) resulting in a computationally intensive algorithm. The numerical solution of Eq. (11) with the boundary conditions (17)–(20) is classified as a boundary value problem (BVP) because the conditions are formulated at the membrane centre ($z = 0$) and ($z = L$). For solving this problem the bvp4c MATLAB™ routine was used.

### 3.3.8. Model calculation results

Since for modelling purposes the membranes were assumed as homogeneous and symmetrical, the values found for the different parameters must be regarded as mean values for the whole membrane. In fact one should expect that the catalytic layer and the selective layer have very different transport properties.

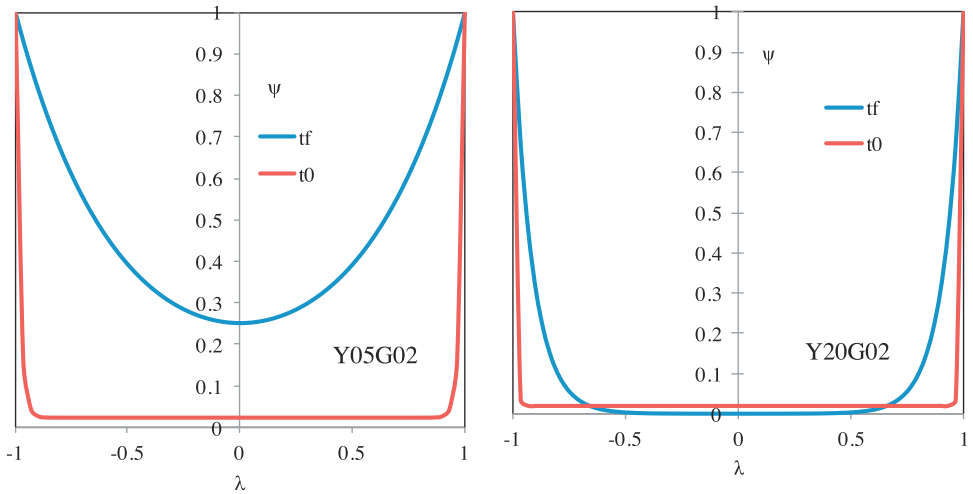


**Fig. 8.** Membrane phenylacetaldehyde concentration profiles calculated assuming symmetrical homogeneous membranes, for the membranes with the lowest (Y05G02) and the highest (Y20G02) zeolite loading, at the initial reaction time ($t_0$) and the final reaction time ($t_f$).

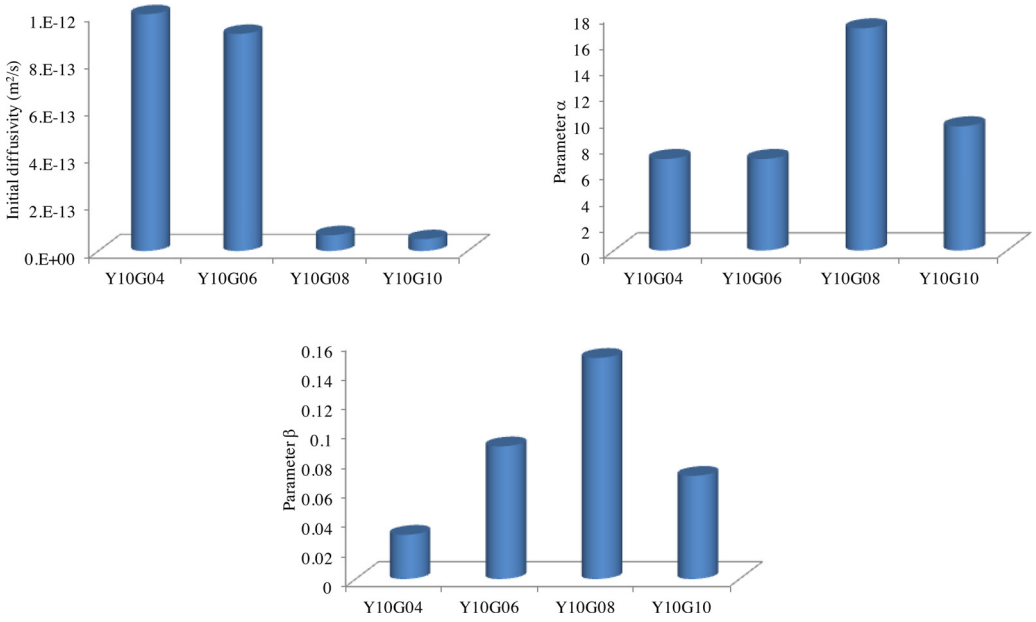


**Fig. 9.** Effect of polymer cross-linking on the model parameters.

*3.3.8.1. Effect of zeolite loading.* The calculated initial diffusivity decreases when the zeolite loading increases (Fig. 7) suggesting that the zeolite particles act as barriers to the transport of the reactants across the membranes. Simultaneously the diffusivity enhancing factor ($\alpha$) also decreases when the zeolite loading increases, suggesting that the H-USY particles limit the polymer chains movements. Parameter $\beta$ shows a maximum at 10% loading, decreasing for higher loadings. A possible interpretation for the induction period (to which $\beta$ is related) is the following: if a spacer is intercalated between the polymer chains the binding of acetal molecules to the PVA OH groups in the close proximity of that spacer becomes ineffective on separating the polymer chains. The length of the induction period corresponds to the "filling" of those ineffective zones which increase with the increase of zeolite loading. However, for higher loadings, the increase of membrane rigidity and the consequent decrease of the ability of diffusivity enhancement leads also to a decrease of the induction period.

Fig. 8 shows the phenylacetaldehyde concentration profiles calculated for the membranes with the lowest (Y05G02) and the highest (Y20G02) zeolite loading, at the initial reaction time ($t_0$) and the final reaction time ($t_f$). It becomes evident that for the lowest catalyst loading there is a significant enhancement of the membrane transport properties while for the highest loading that improvement is not so significant.

*3.3.8.2. Effect of polymer cross-linking.* Similarly to what was observed for the effects of zeolite loading initial diffusivity also

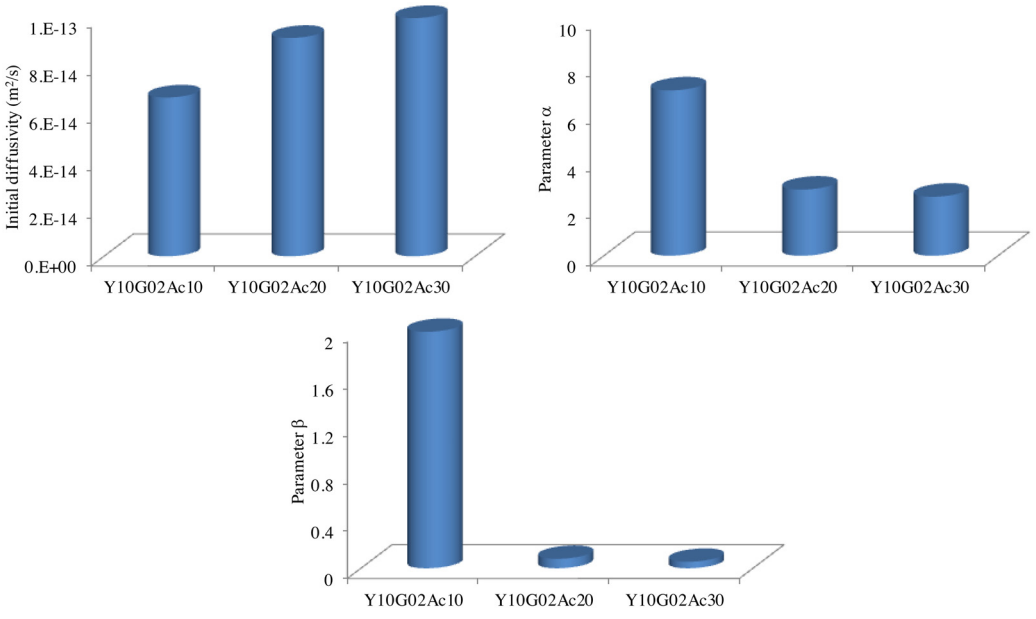


**Fig. 10.** Effect of polymer acetylation on the model parameters.

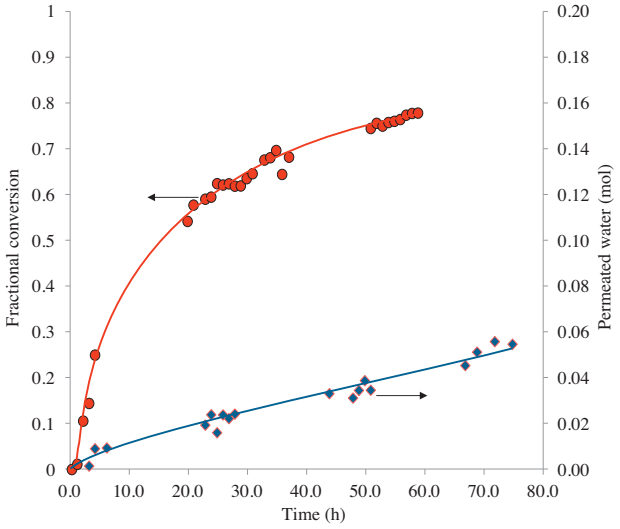


**Fig. 11.** Conversion and permeated water profiles obtained in the pervaporation assisted membrane reactor equipped with membrane Y20G02.

decreases when cross-linking increases (Fig. 9) being the explanation also identical to that given above: the cross-linker acts as a barrier hindering the transport of the reactants. However parameters $\alpha$ and $\beta$ behave differently, increasing with cross-linking until a maximum at 8% cross-linking and then decreasing for higher cross-linking degrees. A possible explanation is that for lower cross-linking degrees the cross-linker acts as a spacer facilitating the intercalation of acetal molecules between the polymer chains.

In what concerns parameter $\alpha$, that intercalation separates the polymer chains enhancing the reactants diffusivity. This enhancement increases with cross-linking. The explanation for the behaviour of parameter $\beta$ is similar to that given above: the binding of acetal molecules in the close vicinity of the cross-linker bridges is ineffective for the separation of polymer chains. When cross-linking increases the number of "ineffectiveness" zones also increases. For 10% cross-linking the membrane rigidity explains the decrease of parameters $\alpha$ e $\beta$.

*3.3.8.3. Effect of polymer acetylation.* When the polymer acetylation increases the calculated initial diffusivity decreases (Fig. 10). This is an unexpected result because it would be expectable that the decrease in interchain hydrogen bridging due to the blocking of PVA OH groups by acetyl groups, would lead to the improvement of the membranes' transport properties. A possible explanation is the decrease of hydrogen binding between the glycerol molecules and the PVA OH groups. As glycerol itself can also act as a spacer keeping the polymer chains apart from each other, the decrease in the number of PVA OH groups leads to the decrease in the number of glycerol molecules bonded to the polymer chains. Consequently the polymer chains would become closer to each other explaining the decrease in initial diffusivity. Although the glycerol swelling results are somewhat erratic, a decrease in the swelling degree seems to take place when the acetylation degree increases (Table 1), giving some support to the above hypothesis.

Parameter $\alpha$ decreases when acetylation increases because the number of OH groups available for hydrogen bonding decreases and therefore decreases the intercalation of acetal molecules.

### 3.4. Catalytic membrane reactor experiments

In order to check if pervaporation takes place, a preliminary test was carried out in a membrane reactor assembled with a PVA membrane loaded with 20% H-USY and with 2% cross-linking (Y20G02), working as described in Section 2.3. Fig. 11 shows the profiles of phenylacetaldehyde conversion and permeated water. The observed initial induction period is likely to be due to the acetal interaction with the polymer matrix as mentioned above. The amount of permeated water was calculated from the amount of acetic acid formed in the permeated solution (acetic anhydride). Phenylacetaldehyde or glycerol esters were not detected in this solution, showing the good selectivity of the membrane to water.

A more detailed study in membrane reactor in which low grade glycerol is used, is being carried out and will be reported in a future work.

## 4. Conclusions

PVA membranes loaded with H-USY were successfully cross-linked with glutaraldehyde and have shown good catalytic activity in the acetalization reaction of phenylacetaldehyde with glycerol.

The modification of zeolite loading, polymer cross-linking or polymer acetylation allow the tuning of the membranes' transport properties.

A diffusion-kinetic model assuming a dependence of phenylacetaldehyde diffusivity on acetal concentration fits quite well the kinetic data.

The results from the experiment carried out in a catalytic membrane reactor operating under sweep gas pervaporation conditions point out the good selectivity of the membrane to water and show that the implementation of the reaction and separation in a single step is feasible.

## Acknowledgements

This work has been supported by national funds through Fundação para a Ciência e a Tecnologia, Ministério da Educação e Ciência (FCT-MEC) under PEst-C/EQB/LA0006/2011 and PTDC/CTM-POL/114579/2009 projects, and grant SFRH/BPD/26961/2006.

## References

[1] M.J. Climent, A. Corma, A. Velty, Appl. Catal., A 263 (2004) 155–161.
[2] E. Santacesaria, G. Martinez Vicente, M. Di Serio, R. Tesser, Catal. Today 195 (2012) 2–13.
[3] Y. Zheng, X. Chen, Y. Shen, Chem. Rev. 108 (2008) 5253–5277.
[4] N. Rahmat, A.Z. Abdullah, A.R. Mohamed, Renewable Sustainable Energy Rev. 14 (2010) 987–1000.
[5] P. Ferreira, I.M. Fonseca, A.M. Ramos, J. Vital, J.E. Castanheiro, Appl. Catal., B 91 (2009) 416–422.
[6] P. Ferreira, I.M. Fonseca, A.M. Ramos, J. Vital, J.E. Castanheiro, Appl. Catal., B 98 (2010) 94–99.
[7] M.R. Capeletti, L. Balzano, G. de la Puente, M. Laborde, U. Sedran, Appl. Catal., A 198 (2000) L1–L4.
[8] S.P. Chopade, M.M. Sharma, React. Funct. Polym. 34 (1997) 37–45.
[9] I. Vankelecom, Chem. Rev. 102 (2002) 3779–3810.
[10] M.G. Buonomenna, S.H. Choi, E. Drioli, Asia-Pac. J. Chem. Eng. 5 (2010) 26–34.
[11] B. Van der Bruggen, Pervaporation membrane reactors, in: E. Drioli, L. Giorno (Eds.), Comprehensive Membrane Science and Engineering, 3, Elsevier B.V., Kindlington, 2010, pp. 135–163.
[12] D.J. Benedict, S.J. Parulekar, S.P. Tsai, Esterification of lactic acid and ethanol with/without pervaporation, Ind. Eng. Chem. Res. 42 (2003) 2282–2291.
[13] G. Bengtson, M. Oehring, D. Fritsch, Chem. Eng. Process. 43 (2004) 1159–1170.
[14] M.T. Sanz, J. Gmehling, Esterification of acetic acid with isopropanol coupled with pervaporation: Part I: kinetics and pervaporation studies, Chem. Eng. J. 123 (2006) 1–8.
[15] I. Agirre, M.B. Guemez, H.M. van Veen, A. Motelica, J.F. Vente, P.L. Arias, J. Membr. Sci. 371 (2011) 179–188.
[16] V.S. Praptowidodo, J. Mol. Struct. 739 (2005) 207–212.
[17] J.E. Castanheiro, I.M. Fonseca, A.M. Ramos, R. Oliveira, J. Vital, Catal. Today 104 (2005) 296–304.
[18] H.S. Mansur, C.M. Sadahira, A.N. Souza, A.A.P. Mansur, Mater. Sci. Eng. 28 (2008) 539–548.
[19] A. Hernández, P. Prádanos, L. Palacio, R. Recio, A. Marcos-Fernández, A. Lozano, Scanning probe microscopy techniques in the investigation of homogeneous and heterogeneous dense membranes: the case for gas separtion membranes,

in: C. Güell, M. Ferrando, F. López (Eds.), Monitoring and Visualizing Membrane-Based Processes, Wiley-VCH, Weinheim, 2009, p. 91.
[20] J. Vital, A.M. Ramos, I.F. Silva, J.E. Castanheiro, Catal. Today 67 (2001) 217.
[21] J.E. Castanheiro, A.M. Ramos, I.M. Fonseca, J. Vital, Appl. Catal., A 311 (2006) 17–23.
[22] L. Guerreiro, P.M. Pereira, I.M. Fonseca, R.M. Martin-Aranda, A.M. Ramos, J.M.L. Dias, R. Oliveira, J. Vital, Catal. Today 156 (2010) 191–197.
[23] S. Wu, J.-E. Gallot, M. Bousmina, C. Bouchard, S. Kaliaguine, Catal. Today 56 (2000) 113.
[24] A. Yawalkar, V. Pangarkar, G. Baron, J. Membr. Sci. 182 (2001) 129–137.
[25] J.M. Sousa, P. Cruz, A. Mendes, Catal. Today 67 (2001) 281.
[26] J.M. Sousa, P. Cruz, A. Mendes, J. Membr. Sci. 181 (2001) 241.
[27] E. Nagy, Ind. Eng. Chem. Res. 46 (2007) 2295–2306.
[28] J.R. Kittrell, Adv. Chem. Eng. 8 (1970) 97.